Int. J. Electrochem. Sci., 8 **(2013)** 435 - 445

International Journal of
ELECTROCHEMICAL
SCIENCE
www.electrochemsci.org

Electro-oxidation of Ethanol on PtPdSn/C-Sb_2O_5.SnO_2 Electrocatalysts Prepared by Borohydride Reduction

R.M.Piasentin[1], *R.F.B. de Souza*[1], *J.C.M. Silva*[2], *E.V. Spinacé*[1], *M.C. Santos*[2] *and A.O. Neto*[1,*]

[1] Instituto de Pesquisas Energéticas e Nucleares, IPEN/CNEN-SP, Av. Prof. Lineu Prestes, 2242 Cidade Universitária, CEP 05508-900,São Paulo, SP, Brazil
[2] LEMN - Laboratório de Eletroquímica e Materiais Nanoestruturados, CCNH - Centro de Ciências Naturais e Humanas, UFABC - Universidade Federal do ABC, CEP 09.210-170, Rua Santa Adélia 166, Bairro Bangu, Santo André, SP, Brazil
[*]E-mail: aolivei@ipen.br

Received: 3 October 2012 / *Accepted:* 22 November 2012 / *Published:* 1 January 2013

Pt/C-Sb_2O_5.SnO_2, PtPd/C-Sb_2O_5.SnO_2 and PtPdSn/C-Sb_2O_5.SnO_2 electrocatalysts were prepared in a single step using $H_2PtCl_6.6H_2O$, $Pd(NO_3)_2.2H_2O$ and $SnCl_2.2H_2O$ as metal sources, sodium borohydride as reducing agent and a physical mixture of 85% Vulcan Carbon XC72 and 15% Sb_2O_5.SnO_2 (antimony tin oxide – ATO) as support. X-ray diffractograms showed that Pt-Pd-Sn(fcc) alloy, carbon and Sb_2O_5.SnO_2 phases are present in the PtPdSn/C-Sb_2O_5.SnO_2 electrocatalysts. Transmission electron microscopy for all electrocatalysts showed that the metal nanoparticles were homogeneously distributed over the supports with average particle sizes in the range of 3-5 nm. The electro-oxidation of ethanol was studied by cyclic voltammetry and chronoamperometry at 25°C and in a single Direct Ethanol Fuel Cell (DEFC) at 100°C. PtPdSn/C-Sb_2O_5.SnO_2 electrocatalysts exhibited superior performance for ethanol electro-oxidation than PtPd/C-Sb_2O_5.SnO_2 and Pt/C-Sb_2O_5.SnO_2 electrocatalysts, respectively. *In situ* FTIR studies showed that acetic acid and CO_2 are preferentially formed using PtPdSn/C-Sb_2O_5.SnO_2 electrocatalysts.

Keywords: PtPdSn/C-Sb2O5.SnO2 electrocatalysts, ethanol electro-oxidation, fuel cell, FTIR spectroscopy.

1. INTRODUCTION

Methanol and ethanol have been the most studied alcohols for Direct Alcohol Fuel Cell (DAFC) application due to their low cost, low pollutant emissions and high theoretical energy density [1-6]. Ethanol has been considered more interesting as fuel in DAFCs due to its renewability, low toxicity, safety, high energy density, and its easy production in great quantities from biomass [1-6].

Platinum electrocatalyst is commonly used as anode or cathode in direct alcohol fuel cell, however it is easily poisoned by the products of oxidation of organic molecules, such as carbon monoxide [7-9]. An alternative is the addition of a co catalysts to platinum, where the bi-metallic catalysts containing Pt could be more active as anode catalysts than Pt alone due to the so-called bi-functional mechanism [10-13].

PtSn binary electrocatalysts have been considered as the most active electrocatalysts for ethanol electro-oxidation but, due to the difficulty of C–C bond breaking, the main products formed are acetaldehyde and acetic acid. Thus, the addition of a third metallic element to PtSn could improve the performance for ethanol electro-oxidation [14]. Spinace *et al* [15] showed that the addition of Rh to PtSn/C electrocatalysts improved the performance of a Direct Ethanol Fuel Cell (DEFC); however it was observed that acetic acid was the principal product formed on Rh-modified PtSn/C electrodes and for that reason it is necessary to design new catalysts that enables the complete electro-oxidation of ethanol to CO_2.

Recently, PtPd electrocatalysts have been proposed as an ethanol tolerant oxygen reduction catalyst [16] and exhibited a high resistance against CO poisoning coming from the oxidation of formic acid and methanol [16]. Besides this, the use of Pd in binary and ternary electrocatalysts is also very interesting because the high cost of Pt limits its use in DEFC and Pd is at least 50 times more abundant on the earth than Pt [17-18].

The use of PtPdSn/C has been proposed as a second alternative to increase the performance of the electrocatalysts for ethanol electro-oxidation, however PtSnPd/C (1:1:0.3 and 1:1:1) electrocatalysts synthesized by a formic acid reduction method showed lower activity for ethanol oxidation in comparison with binary PtSn/C [19]. This result could indicate that both activity and selectivity of PtSnPd/C depends strongly on the catalyst preparation method which could lead to different species present on the surface of the obtained materials [19].

A third alternative to increase the performance of the electrocatalysts for ethanol electro-oxidation has been the deposit of Pt on the surface of metal oxides such as CeO_2, RuO_2 or SnO_2 [20-21], however, these oxides have poor electron conductivity at low temperatures. Recently, it has been proposed that the use of SnO_2 doped with Sb ($Sb_2O_5.SnO_2$, ATO), which has an enhancement of electrical conductivity compared with SnO_2, CeO_2 or others oxides [22-24].

The enhancement of activity for Pt/C-$Sb_2O_5.SnO_2$ electrocatalysts could be attributed to better dispersion of Pt particles on the ATO support, as well as to the effects of SnO_2 adjacent to Pt (bifunctional effect and/or the electronic effect) and a presence of Sb_2O_5 could also enhance the electron conductivity.

In this context, the aim of this work was to prepare PtPdSn/C-$Sb_2O_5.SnO_2$ electrocatalysts by borohydride reduction and to test these electrocatalysts for ethanol electro-oxidation in acidic medium by cyclic voltammetry, chronoamperometry and in a single DEFC. The mechanism of ethanol oxidation on PtPdSn/C-Sb_2O_5 electrocatalysts was also investigated *in situ* by FTIR spectroscopy to obtain information about intermediates and reaction products formed.

2. EXPERIMENTAL

Pt/C-Sb_2O_5.SnO_2, Pd/C-Sb_2O_5.SnO_2, PtPd/C-Sb_2O_5.SnO_2 (Pt:Pd atomic ratio of 80:20) and PtPdSn/C-Sb_2O_5.SnO_2 (20 wt.% of metals loading; Pt:Pd:Sn atomic ratios of 90:05:05 and 80:10:10) electrocatalysts were prepared using $Pd(NO_3)_2.2H_2O$, $H_2PtCl_6 \cdot 6H_2O$ and $SnCl_2.2H_2O$ as metal sources, sodium borohydride as reducing agent and a physical mixture of 85% Vulcan Carbon XC72 and 15% Sb_2O_5.SnO_2 (ATO) as support. The Pt:Pd ratio atomic composition of the PtPd/C-Sb_2O_5.SnO_2 electrocatalysts was chosen to be 80:20 since it was observed in a previous work that is was the most active ratio atomic composition for ethanol electro-oxidation [2].

X-ray diffraction (XRD) analyses were performed using a Rigaku diffractometer model Miniflex II using Cu Kα radiation source (l = 0.15406 nm). The diffractograms were recorded from 2θ = 20° to 90° with a step size of 0.05° and a scan time of 2s per step.

Transmission electron microscopy (TEM) was carried using a JEOL JEM-2100 electron microscope operated at 200 kV. The mean nanoparticle sizes were determined by counting more than 200 particles from different regions of each sample.

The cyclic voltammetry and chronoamperommetry measurements were carried out at 25^{o}C using a Microquimica potentiostat, whose working electrodes (geometric area of 0.3 cm^2 with a depth of 0.3 mm) were prepared using the thin porous coating technique [22]. The reference electrode was a reversible hydrogen electrode (RHE) and the counter electrode was a Pt plate. The electrochemical measurements were realized in presence of 1.0 mol L^{-1} of ethanol in 0.5 mol L^{-1} H_2SO_4 solutions saturated with N_2.

Direct ethanol fuel cell tests were performed using Pt/C, Pt/C-Sb_2O_5.SnO_2, PtPd/C-Sb_2O_5.SnO_2 and PtPdSn/C-Sb_2O_5.SnO_2 electrocatalysts as anode and Pt/C electrocatalysts as cathode in a single cell with an area of 5 cm^2. For direct ethanol fuel cell studies the teflon treated carbon-cloth was utilized as a gas diffusion layer and a Nafion 117® membrane as electrolyte. The experimental procedure was realized in accordance with reference 22.

The spectroelectrochemical ATR-FTIR *in situ* measurements were performed with a Varian® 660 IR spectrometer equipped with a MCT detector cooled with liquid N_2, ATR accessory (MIRacle with a Diamond/ ZnSe Crystal Plate Pike®) and a special cell [10]. The working electrodes were prepared in accordance with reference 10 and these experiments were performed at 25^{o}C in presence of 0.1 mol L^{-1} $HClO_4$ in 1.0 mol L^{-1} ethanol. The absorbance spectra were collected as the ratio $R:R_0$, where R represents a spectrum at a given potential and R_0 is the spectrum collected at 0.05 V. The positive and negative directional bands represent, respectively, the gain and the loss of species at the sampling potential. The spectra were computed from 128 interferograms averaged from 2500 cm^{-1} to 850 cm^{-1} with the spectral resolution set to 4 cm^{-1}. Initially, a reference spectrum (R_0) was measured at 0.05 V, and the sample spectra were collected after applying successive potential steps from 0.2 V to 1.0 V [10].

3. RESULTS AND DISCUSSION

The X-ray diffractograms of Pt/C-Sb_2O_5.SnO_2, Pd/C-Sb_2O_5.SnO_2, PtPd/C-Sb_2O_5.SnO_2 (80:20), PtPdSn/C-Sb_2O_5.SnO_2 (80:10:10) and PtPdSn/C-Sb_2O_5.SnO_2 (90:05:05) electrocatalysts are shown in

Fig. 1. All diffractograms showed a broad peak at about 25º associated with the Vulcan XC72 support and four peaks at approximately 2θ = 40º, 47º, 67º and 82º, which are associated with the (111), (200), (220) and (311) planes, respectively, of the fcc structure characteristic of Pt, Pd or Pt-Pd alloys [2]. For all electrocatalysts were observed peaks at about 2θ = 27º, 34º, 38º, 52º, 55º, 62º, 65º and 66º, which were characteristic of $Sb_2O_5.SnO_2$ (ATO) used as support [2].

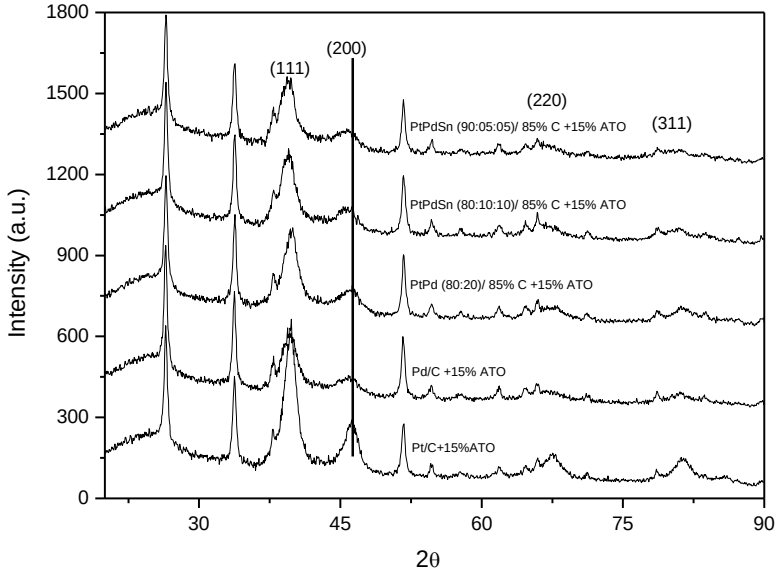

Figure 1. X-ray diffractograms of the Pt/C-$Sb_2O_5.SnO_2$, Pd/C-$Sb_2O_5.SnO_2$, PtPd/C-$Sb_2O_5.SnO_2$ (80:20), PtPdSn/C-$Sb_2O_5.SnO_2$ (80:10:10) and PtPdSn/C-$Sb_2O_5.SnO_2$ (90:05:05).

Comparing with PtPd/C-$Sb_2O_5.SnO_2$ electrocatalyst, the (200) peak of the Pt-Pd(fcc) phase of the PtPdSn/C-$Sb_2O_5.SnO_2$ electrocatalysts was shifted to lower 2θ values indicating an alloy formation between Pt, Pd and Sn. Similar results were described by Antoline *et al* [19] that also observed for PtPdSn electrocatalysts the incorporation of Sn atoms into the Pt-Pd(fcc) lattice. The mean crystallite sizes determined using Scherrer equation for all electrocatalysts were in the range of 3-4 nm, which were similar to the ones described in the literature [2, 19].

Fig. 2A-E present TEM micrographs and size distributions (histograms) of the following electrocatalysts: Pt/C-$Sb_2O_5.SnO_2$ (A), Pd/C-$Sb_2O_5.SnO_2$ (B), PtPd/C-$Sb_2O_5.SnO_2$ (80:20) (C), PtPdSn/C-$Sb_2O_5.SnO_2$ (80:10:10) (D) and PtPdSn/C-$Sb_2O_5.SnO_2$ (90:05:05) (E).

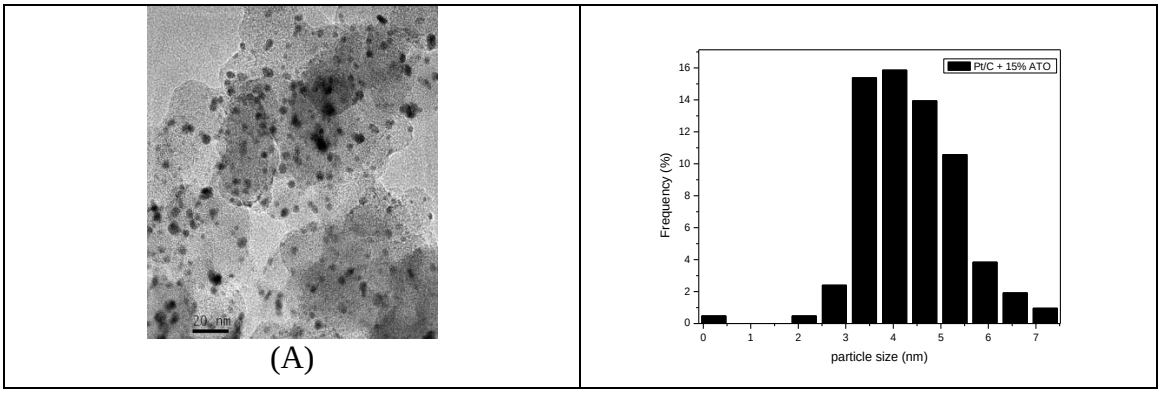

(A)

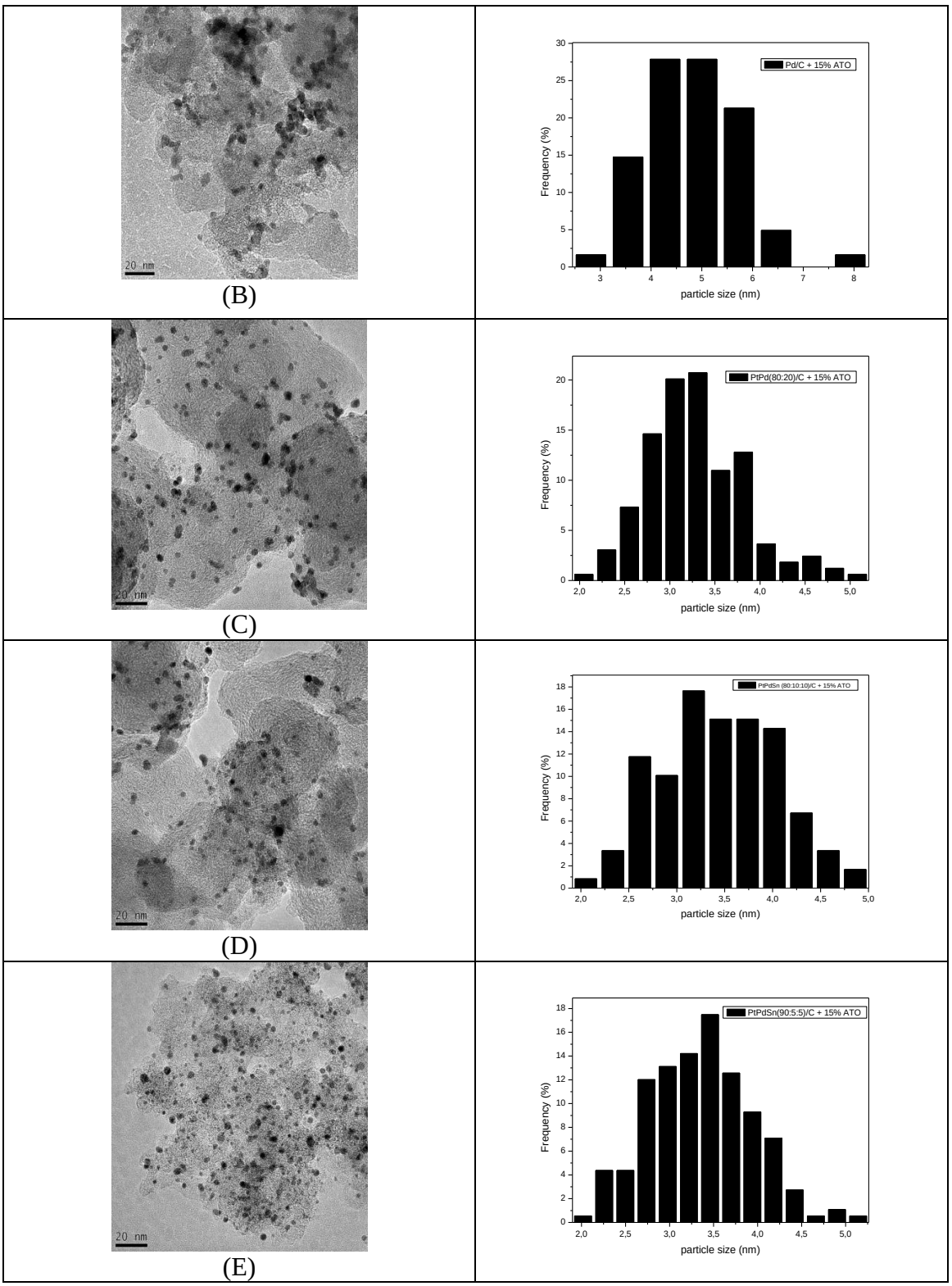

Figure 2. TEM micrograph and a histogram of (2A) Pt/C-Sb_2O_5.SnO_2, (2B) Pd/C-Sb_2O_5.SnO_2, (2C) PtPd/C-Sb_2O_5.SnO_2 (80:20), (2D) PtPdSn/C-Sb_2O_5.SnO_2 (80:10:10) and (2E) PtPdSn/C-Sb_2O_5.SnO_2 (90:05:05).

PtPd/C-Sb_2O_5.SnO_2 (80:20), PtPdSn/C-Sb_2O_5.SnO_2 (80:10:10) and PtPdSn/C-Sb_2O_5.SnO_2 (90:05:05) showed average particle sizes of 3.0±0.5 nm, while for Pt/C-Sb_2O_5.SnO_2 and Pd/C-

$Sb_2O_5.SnO_2$ average particle sizes of 4.0±1.0 nm were observed. For all electrocatalysts it was observed a good distribution of the nanoparticles on the carbon support. Fig. 3 shows the cyclic voltammograms of all electrocatalysts prepared at 25°C in presence of 1.0 mol L^{-1} ethanol in 0.5 mol L^{-1} H_2SO_4.

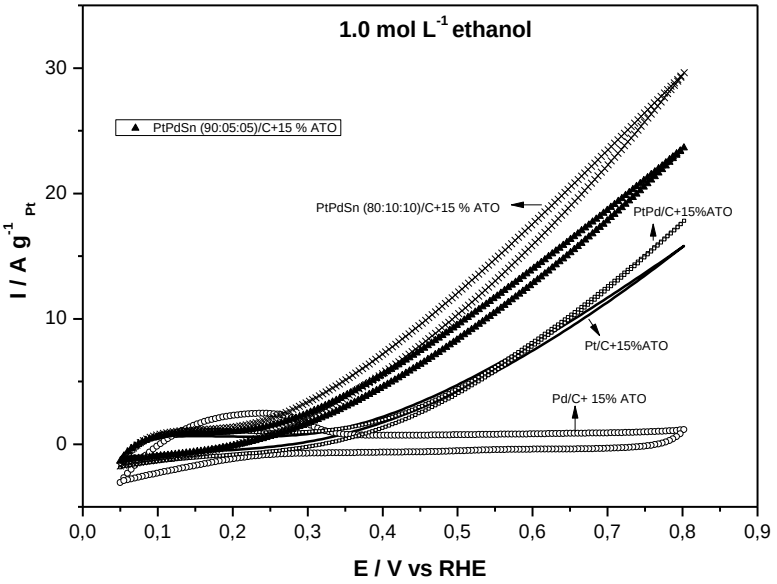

Figure 3. Cyclic voltammograms of the Pt/C-$Sb_2O_5.SnO_2$, Pd/C-$Sb_2O_5.SnO_2$, PtPd/C-$Sb_2O_5.SnO_2$ (80:20), PtPdSn/C-$Sb_2O_5.SnO_2$ (80:10:10) and PtPdSn/C-$Sb_2O_5.SnO_2$ (90:05:05) electrocatalysts at 25°C in 1 mol L^{-1} ethanol solution in 0.5 mol L^{-1} H_2SO_4 with a sweep rate of 10 mV s^{-1}.

The ethanol electro-oxidation started at approximately 0.25 V for PtPdSn/C-$Sb_2O_5.SnO_2$ electrocatalysts whereas for PtPd/C-$Sb_2O_5.SnO_2$ and Pt/C-$Sb_2O_5.SnO_2$ electrocatalysts it started at about 0.4 V (+150 mV). Pd/C-$Sb_2O_5.SnO_2$ showed lower currents in comparison to the others electrocatalysts showing that it is practically inactive for ethanol oxidation in acidic medium as already observed by Piasentin *et al* [2]. This is an indication that the adsorption of ethanol does not occur on Pd sites. The best performance of PtPdSn/C-$Sb_2O_5.SnO_2$ electrocatalysts for ethanol oxidation could be attributed as a result of the combination of Pt, Pd, Sn and ATO, which constitutes the electrocatalyst. It is known that ATO or Sn reacts with H_2O and provides OH species to oxidize the intermediates formed on ethanol electro-oxidation at Pt or Pd sites, while Pt facilitates ethanol dehydrogenation [15]. On the other hand, Antoline *et al* [19] showed that the ternary PtSnPd catalyst had a lower activity for ethanol electro-oxidation than the binary PtSn catalyst prepared by formic acid reduction of the metal precursors showing that the performance of the PtPdSn electrocatalysts for ethanol electro-oxidation depends strongly on the catalyst preparation methodology and on their constituents.

Fig. 4 shows the current-time curves for ethanol electro-oxidation for all electrocatalysts at 25°C in the potential of 0.5 V for 30 min.

For Pd/C-Sb_2O_5.SnO_2 electrocatalysts a great initial current drop was observed and a very low performance for ethanol oxidation in comparison with the others electrocatalysts.

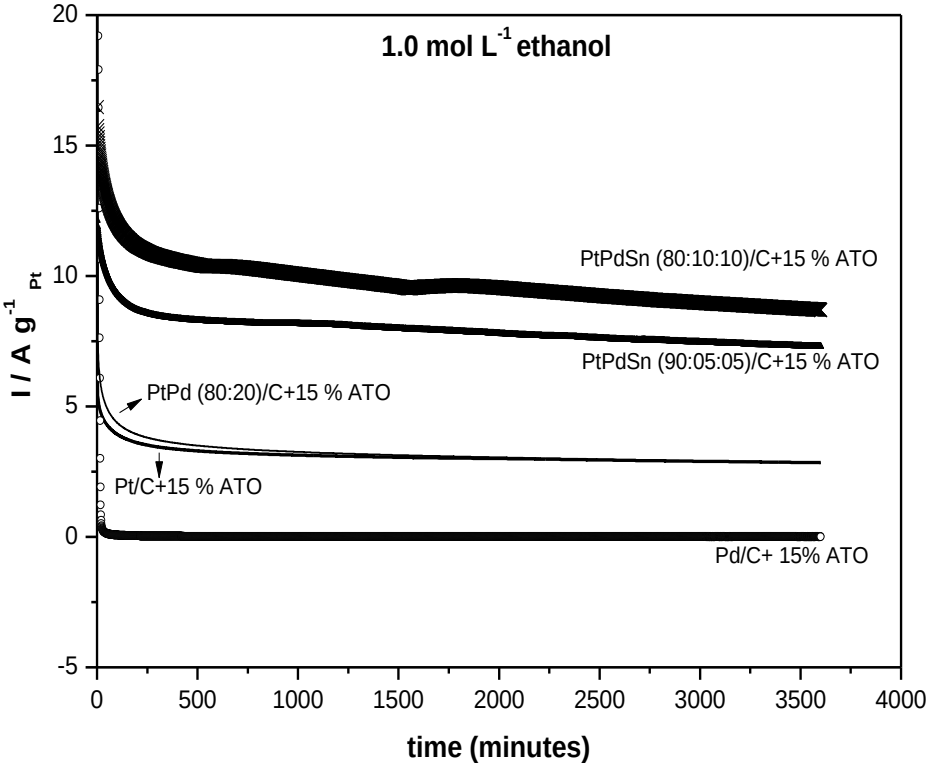

Figure 4. Current-time curves at 0.5 V in 1 mol L^{-1} ethanol solution in 0.5 mol L^{-1} H_2SO_4 for Pt/C-Sb_2O_5.SnO_2, Pd/C-Sb_2O_5.SnO_2, PtPd/C-Sb_2O_5.SnO_2 (80:20), PtPdSn/C-Sb_2O_5.SnO_2 (80:10:10) and PtPdSn/C-Sb_2O_5.SnO_2 (90:05:05) electrocatalysts at 25°C.

Pt/C-Sb_2O_5.SnO_2 and PtPd/C-Sb_2O_5.SnO_2 electrocatalysts showed similar performance for ethanol oxidation. The current values obtained for PtPdSn/C-Sb_2O_5.SnO_2 electrocatalysts were higher than those obtained for Pt/C-Sb_2O_5.SnO_2 and PtPd/C-Sb_2O_5.SnO_2 electrocatalysts in agreement with cyclic voltammetry experiments. The final current values at 0.5 V (T= 25°C) increase in the following order: PtPdSn/C-Sb_2O_5.SnO_2 (80:10:10) > PtPdSn/C-Sb_2O_5.SnO_2 (90:05:05) > PtPd/C-Sb_2O_5.SnO_2 (80:20) ≈ Pt/C-Sb_2O_5.SnO_2 > Pd/C-Sb_2O_5.SnO_2.

Fig. 5 shows the performances of a single DEFC using Pt/C, Pt/C-Sb_2O_5.SnO_2, PtPd/C-Sb_2O_5.SnO_2 (80:20), PtPdSn/C-Sb_2O_5.SnO_2 (80:10:10) and PtPdSn/C-Sb_2O_5.SnO_2 (90:05:05) as anode electrocatalysts. PtPdSn/C-Sb_2O_5.SnO_2 (80:10:10 and 90:05:05) electrocatalysts showed higher values of maximum power density (50 $mWcm^{-2}$) in comparison with Pt/C-Sb_2O_5.SnO_2 (37 $mWcm^{-2}$), PtPd/C-Sb_2O_5.SnO_2 (30 $mWcm^{-2}$) and Pt/C (8 $mWcm^{-2}$). The experiments at 100°C on single DEFC also showed that the addition of Sn into PtPd/C-Sb_2O_5.SnO_2 electrocatalyst can promote its activity for ethanol electro-oxidation.

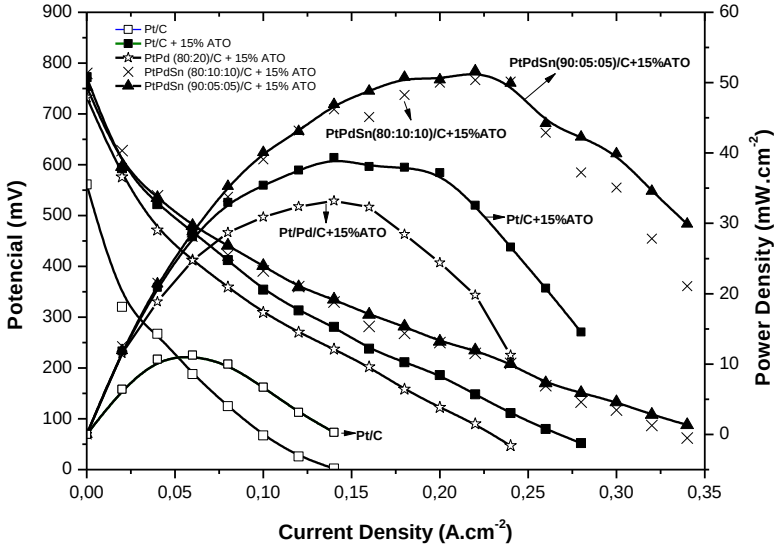

Figure 5. I–V curves and the power density at 100 °C of a 5 cm^2 DEFC using Pt/C, Pt/C-Sb_2O_5.SnO_2, PtPd/C-Sb_2O_5.SnO_2 (80:20), PtPdSn/C-Sb_2O_5.SnO_2 (80:10:10) and PtPdSn/C-Sb_2O_5.SnO_2 (90:05:05) electrocatalysts as anode (1 mg_{Pt} cm^{-2} catalyst loading) and Pt/C E-TEK electrocatalyst cathode (1 mg_{Pt} cm^{-2} catalyst loading, 20 wt.% Pt loading on carbon), Nafion® 117 membrane, ethanol (2.0 mol L^{-1}) and oxygen pressure (2 bar).

The highest catalytic activity of PtPdSn/C-Sb_2O_5.SnO_2 could be attributed to the synergy between the constituents of the electrocatalyst. It could be associated a change in the Pt electronic density (electronic effect) associated with the formation of Pt-Pd-Sn alloys that also favors a bifunctional mechanism in which Pt affects ethanol adsorption and dissociation and Sn and/or ATO provides oxygenated species for the oxidative removal of the adsorbed intermediates formed during ethanol electro-oxidation [25].

Fig. 6A-E show *in situ* FTIR spectra collected at different potentials for ethanol electro-oxidation using the following electrocatalysts: Pt/C (A), Pt/C-Sb_2O_5.SnO_2 (B), PtPd/C-Sb_2O_5.SnO_2 (80:20) (C), PtPdSn/C-Sb_2O_5.SnO_2 (80:10:10) (D) and PtPdSn/C-Sb_2O_5.SnO_2 (90:05:05) (E).

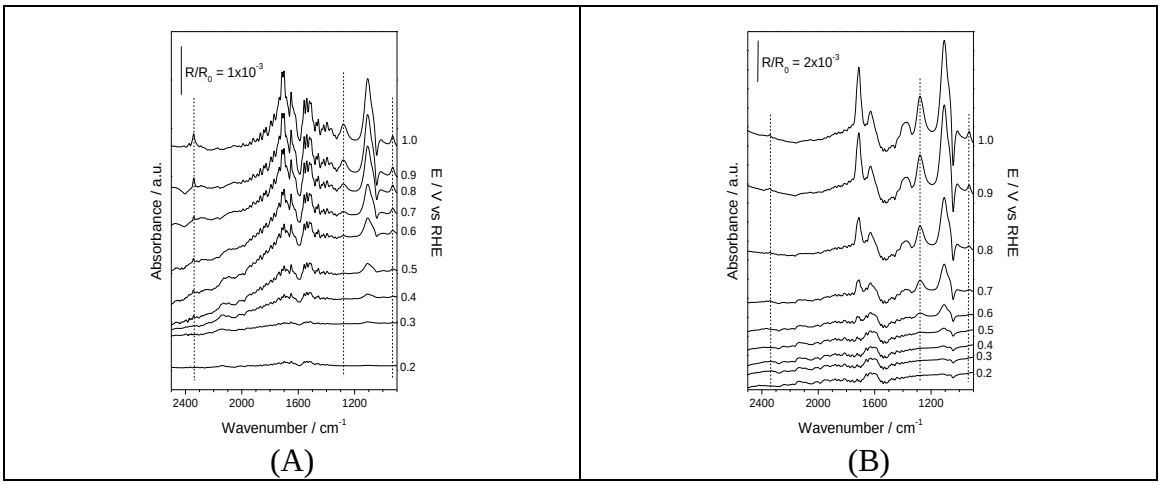

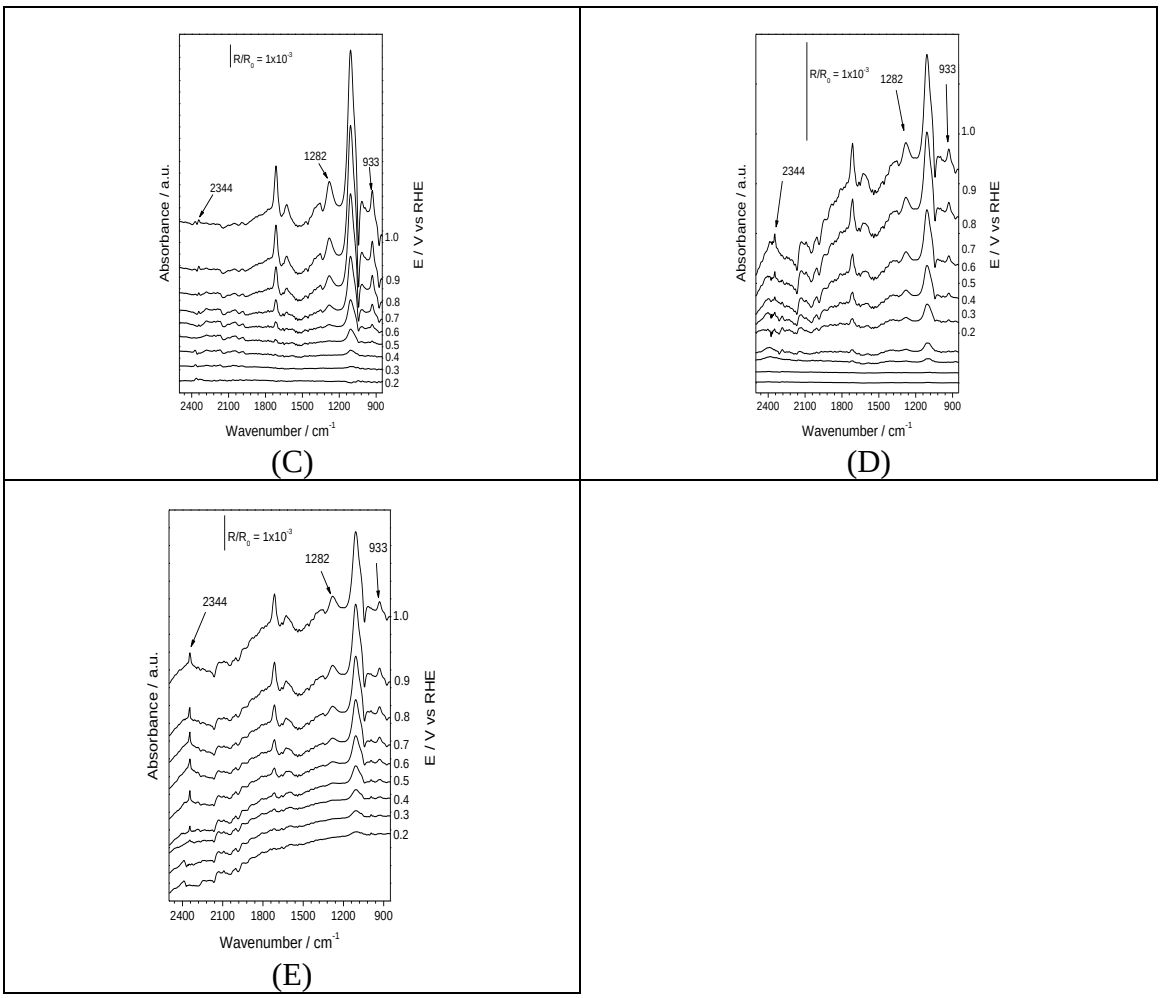

Figure 6. In situ FTIR spectra taken at several potentials (indicated) in 0.1 mol L^{-1} $HClO_4$ + 1.0 mol L^{-1} ethanol for (A) Pt/C, (B) Pt/C-Sb_2O_5.SnO_2, (C) PtPd/C-Sb_2O_5.SnO_2 (80:20), (D) PtPdSn/C-Sb_2O_5.SnO_2 (80:10:10) and (E) PtPdSn/C-Sb_2O_5.SnO_2 (90:05:05). The backgrounds were collected at 0.05 V (RHE scale) with a sweep rate of 1 mV s^{-1}.

The spectra were taken at different potentials (0.2 V to 1.0 V) in the presence of 0.1 mol L^{-1} $HClO_4$ in 1 mol L^{-1} ethanol. These experiments were carried out in accordance with reference [10].

The main bands in the FTIR spectra were observed at 2344, 1282 and 933 cm^{-1}, which are characteristic of the presence of CO_2, acetic acid and acetaldehyde [10].

Fig. 7 shows the normalized integrated band intensities in function of the potential for acetaldehyde (7a), acetic acid (7b) and CO_2 (7c) generated during ethanol electro-oxidation for Pt/C, Pt/C-Sb_2O_5.SnO_2, PtPd/C-Sb_2O_5.SnO_2 (80:20), PtPdSn/C-Sb_2O_5.SnO_2 (80:10:10) and PtPdSn/C-Sb_2O_5.SnO_2 (90:05:05) electrocatalysts. For comparison, the intensities were normalized by intensity measured at 1.0 V for each band. It was observed that for Pt/C the production of acetaldehyde starts 0.2 V followed by formation of acetic acid and CO_2, which only started close to 0.5 V. However, it is possible to observe for all electrocatalysts containing ATO that the acetaldehyde production shifted to more positive potentials while the acetic acid production beginning at lower potentials than Pt/C. In fact, this evidence may indicate that ATO can provides oxygen containing species to oxidize

acetaldehyde to acetic acid or oxidize ethanol directly to acetic acid at low potentials in a similar manner already observed for electrocatalysts using mixtures of carbon and oxides as support [21,26]. The most active materials for ethanol electro-oxidation (PtPdSn/C-Sb_2O_5.SnO_2 (80:10:10) and PtPdSn/C-Sb_2O_5.SnO_2 (90:05:05) contain Sn as Pt-Pd-Sn (fcc) alloys. For both electrocatalysts the production of acetic acid and CO_2 between 0.3 and 0.7 V were superior to the electrocatalysts that does not contain Sn in the alloy.

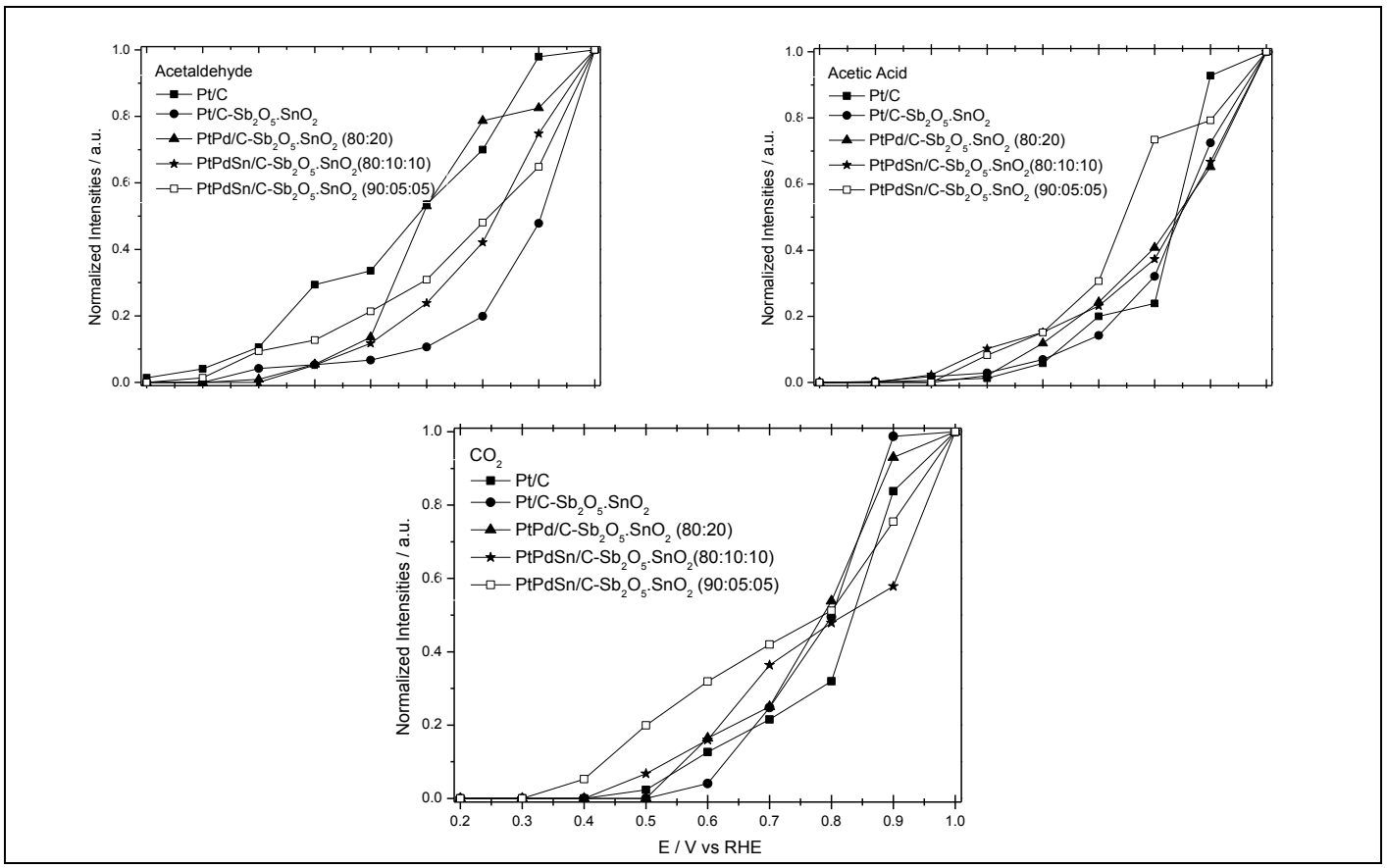

Figure 7. Integrated CO_2, acetic acid and acetaldehyde band intensity as a function of the electrode potential for: Pt/C, Pt/C-Sb_2O_5.SnO_2, PtPd/C-Sb_2O_5.SnO_2 (80:20), PtPdSn/C-Sb_2O_5.SnO_2 (80:10:10) and PtPdSn/C-Sb_2O_5.SnO_2 (90:05:05). Data extracted from fig. 6.

4. CONCLUSIONS

The borohydride reduction showed to be an effective method to produce Pt/C-Sb_2O_5.SnO_2, PtPd/C-Sb_2O_5.SnO_2 and PtPdSn/C-Sb_2O_5.SnO_2 in a single step for ethanol electro-oxidation. The X-ray diffractograms showed that Pt-Pd-Sn(fcc) alloy, carbon and Sb_2O_5.SnO_2 phases are present in the PtPdSn/C-Sb_2O_5.SnO_2 electrocatalysts. Transmission electron microscopy for all electrocatalysts showed that the metal nanoparticles were homogeneously distributed over the supports with average particle sizes in the range of 3-5 nm. The electrochemical measurements and the experiments in a single DEFC showed that PtPdSn/C-Sb_2O_5.SnO_2 electrocatalysts exhibited superior

performance for ethanol electro-oxidation than PtPd/C-Sb_2O_5.SnO_2 and Pt/C-Sb_2O_5.SnO_2 electrocatalysts. The highest catalytic activity of PtPdSn/C-Sb_2O_5.SnO_2 seems to be related to the combination of the bifunctional mechanism and the electronic effect which lead to the formation of acetic acid and CO_2 as the major products.

ACKNOWLEDGMENTS
The authors thank the Laboratório de Microscopia do Centro de Ciências e Tecnologia de Materiais (CCTM) by TEM measurements, FAPESP (2011/18246-0) and CNPq (470790/2010-5) for the financial support.

References

1. F. Kadirgan, S. Beyhan, T. Atilan, *Int. J. Hydrogen Energy* 34 (2009) 4312.
2. R.M. Piasentin, E.V. Spinacé, M.M. Tusi, A.O. Neto, *Int. J. Electrochem. Sci*, 6 (2011) 2255.
3. E.A. Batista, G.R.P. Malpass, A.J. Motheo, T. Iwasita, *J Electroanal Chem*, 571 (2004) 273.
4. C. Coutanceau, S. Brimaud, C. Lamy, *Electrochim Acta*, 53 (2008) 6865.
5. S. García-Rodríguez, S. Rojas, M.A. Peña, J.L.G. Fierro, S. Baranton, J.M. Léger *Appl. Catal. B*, 106 (2011) 520.
6. G. Dao-Jun, *J. Power Sources*, 196 (2011) 679.
7. J. Seweryn, A. Lewera, *J. Power Sources*, 205 (2012) 264.
8. J.M.S. Ayoub, A.N. Geraldes, M.M. Tusi, E.V. Spinace, A.O. Neto, *Ionics*, 17 (2011) 559.
9. E. Antolini, J. Power Sources 170 (2007) 1.
10. J.C.M Silva, L.S. Parreira, R.F.B. De Souza, M.L. Calegaro, E.V. Spinacé, A.O. Neto, M.C. Santos, *Appl. Catal. B*, 110 (2011) 141.
11. E. Baranova, A. Tavasoli, T. Amir, *Electrocatal.*, 2 (2011) 89.
12. J.M. Sieben, M.M.E. Duarte, *Int. J. Hydrogen Energy*, 36 (2011) 3313.
13. Y. Wang, S. Song, G. Andreadis, H. Liu, P. Tsiakaras, J. Power Sources 196 (2011) 4980.
14. E.V. Spinacé, M. Linardi, A.O. Neto, *Electrochem Commun*, 7 (2005) 365.
15. E.V. Spinacé, R.R. Dias, M. Brandalise, M. Linardi, A.O. Neto, *Ionics*, 16 (2010) 91.
16. W. He, J. Liu, Y. Qiao, Z. Zou, X. Zhang, D.L. Akins, H. Yang, *J. Power Sources*, 195 (2010) 1046.
17. K. Machida, M. Enyo, *J Electrochem Soc*, 134 (1987) 1472.
18. G.Q. Lu, A. Crown, A. Wieckowski, *J Phys Chem B*, 103 (1999) 9700.
19. E. Antolini, F. Colmati, E.R. Gonzalez, *J Power Sources*, 193 (2009) 555.
20. C. Pan, Y. Li, Y. Ma, X. Zhao, Q. Zhang, *J. Power Sources*, 196 (2011) 6228.
21. A.O. Neto , M. Linardi, D.M. dos Anjos, G. Tremiliosi, E.V. Spinace, *J. Appl. Electrochem.*, 39 (2009) 1153.
22. A.O Neto, M. Brandalise, R.R. Dias, J.M.S. Ayoub, A.C. Silva, J.C. Penteado, M. Linardi, E.V. Spinacé, *Int. J. Hydrogen Energy*, 35 (2010) 9177.
23. K.S. Lee, I.S. Park, Y.H. Cho, D.S. Jung, N. Jung, *J. Catal.*, 258 (2008) 143.
24. Ayoub JMS, Crisafulli R, SpinacéE V, Neto AO, *XVIII SIBEE*, 1 (2011) EC:246.
25. R.F.B. De Souza, L.S. Parreira, J.C.M. Silva, F.C. Simões, M.L. Calegaro, J.M. Giz, G.A. Camara, A.O. Neto, M.C. Santos, *Int. J. Hydrogen Energy*, 36 (2011) 11519.
26. R.S. Henrique, R.F.B. De Souza, J.C.M. Silva, J.M.S. Ayoub, R.M. Piasentin, M. Linardi, E.V. Spinacé, M.C. Santos, A.O. Neto, *Int. J. Electrochem. Sci.*, 7 (2012) 2036.

© 2013 by ESG (www.electrochemsci.org)